University of
**Central
Florida**

Title "Low-Absorption Liquid Crystals for Infrared Beam Steering"
Grant # N00014-13-1-0096
UCF Account 65016248

On behalf of Dr. Shin-Tson Wu, we are pleased to submit the attached Interim Research Performance Report with SF 298 due 10/23/13.

For technical concerns, please contact Dr. Wu directly at swu@creol.ucf.edu. For administrative concerns, please contact Arlisia Potter, Contract Manager, at apotter@creol.ucf.edu.

Thank you.

Vicky Ortiz

Vicky Ortiz, M.A.
Coordinator of Research Programs
CREOL, The College of Optics & Photonics
University of Central Florida
407-823-6825 (ph)
407-882-9013 (fax)
vsortiz@creol.ucf.edu

UCF50
1963–2013 YEARS

Enclosure: Interim Report and SF 298

CC Via email: Peter Craig, ONR
                    Elizabth Ford, ONR
CC Via Fed Ex: Defense Technical Information Center
                    ONR Regional Admin Atlanta – N66020
                    Naval Research Laboratory Code 5596

REPORT DOCUMENTATION PAGE

Form Approved
OMB No. 0704-0188

1. REPORT DATE (DD-MM-YYYY)	2. REPORT TYPE	3. DATES COVERED (From - To)
10/22/2013	Interim Research Performance Report	10/263/12-10/23/13

4. TITLE AND SUBTITLE	5a. CONTRACT NUMBER
Low-Absorption Liquid Crystals for Infrared Beam Steering	
	5b. GRANT NUMBER
	N00014-13-1-0096
	5c. PROGRAM ELEMENT NUMBER

6. AUTHOR(S)	5d. PROJECT NUMBER
Dr. Shin-Tson Wu	
	5e. TASK NUMBER
	5f. WORK UNIT NUMBER

7. PERFORMING ORGANIZATION NAME(S) AND ADDRESS(ES)	8. PERFORMING ORGANIZATION REPORT NUMBER
University of Central Florida 12201 Research Parkway, suite 501 Orlando, FL 32826-3246	

9. SPONSORING/MONITORING AGENCY NAME(S) AND ADDRESS(ES)	10. SPONSOR/MONITOR'S ACRONYM(S)
Office of Naval Research 875 North Randolph Street Arlington, VA 22203-1995	ONR 312
	11. SPONSOR/MONITOR'S REPORT NUMBER(S)

12. DISTRIBUTION/AVAILABILITY STATEMENT

Approved for Public Release; Distribution is Unlimited

13. SUPPLEMENTARY NOTES

14. ABSTRACT

The objective of this project is to develop high birefringence (n), large dielectric anisotropy (), and low-loss polar nematic liquid crystal compounds and mixtures for infrared applications, especially in the MWIR spectral region. The performance goals are: n~0.2 (at ~4 m), 5 (at 1 kHz), and absorption coefficient ≤ 5/cm.

15. SUBJECT TERMS

Low absorption, MWIR, chlorinated liquid crystals, fluorination, FTIR, eutectic mixture, deuteration, nematic phase, birefringence, overtone, fundamental mode, combination

16. SECURITY CLASSIFICATION OF:			17. LIMITATION OF ABSTRACT	1B. NUMBER OF PAGES	19a. NAME OF RESPONSIBLE PERSON
a. REPORT	b. ABSTRACT	c. THIS PAGE			Vicky Ortiz
				23	19b. TELEPHONE NUMBER (Include area code) 407-823-6825

Standard Form 29B (Rev. 8/98)
Prescribed by ANSI Std. Z39.18

Low-absorption liquid crystals for infrared beam steering

UCF Account Number: 6501-6248
ONR contract #: N00014-13-1-0096

Prepared for:	ONR Program Manager
	Dr. Peter Criag
	Email: peter.craig@navy.mil
Contract Period:	Oct. 23, 2012 to Jan. 22, 2015
Performance Period:	Oct. 23, 2012 to Oct. 23, 2013
Principal Investigator:	Prof. Shin-Tson Wu
	College of Optics and Photonics
	University of Central Florida
	Orlando, Florida 32816-2700
	Email: swu@ucf.edu
	Tel: 407-823-4763
	Fax: 407-823-6880

Abstract:

The objective of this project is to develop high birefringence (Δn), large dielectric anisotropy ($\Delta\varepsilon$), and low-loss polar nematic liquid crystal compounds and mixtures for infrared applications, especially in the MWIR spectral region. The performance goals are: $\Delta n \sim 0.2$ (at $\lambda \sim 4$ μm), $\Delta\varepsilon \sim 5$ (at 1 kHz), and absorption coefficient $\alpha < 5$/cm. We first analyzed the absorption mechanisms, including fundamental vibration, overtone, and sum frequencies. Fundamental molecular vibration absorption is very strong and we should eliminate those functional groups having strong absorption in the MWIR region, such as -C$\equiv$N, NCS, C$\equiv$C, etc. Next, the overtone of C-O, C-F, CF_2, CF_3 stretching, C-C skeletal stretching and =C-H in-plane-deformation will also appear in the 4-5 μm region. Finally, the sum frequency is difficult to predict because there are several possible combinations. Although the overtone and sum-frequency absorption is 10X weaker, the incurred absorption is still not negligible, especially for a relatively long optical beam path ($\sim$5mm). Based on our molecular design strategies, we synthesized several chlorinated terphenyls, which exhibit much lower absorption than that of our benchmarked 5CB. Saturated LC compounds and alkyl-chain-free quaterphenyl compounds are also investigated for low absorption in different spectral regions. Some low absorption compounds for LWIR and SWIR are also investigated.

Key words: Low absorption, MWIR, chlorinated liquid crystals, fluorination, FTIR, eutectic mixture, deuteration, nematic phase, birefringence, overtone, fundamental mode, combination

1. Objective

The main objective of this program is to develop low-loss liquid crystals for electronic laser beam steering in the infrared region, especially for MWIR. Ideally, a single collimated beam of emissions from multiple lasers covering this broad band would be directed as a single beam with a common beam director. The major advantages of such a non-mechanical beam steering device are threefold: 1) reduction of system size-weight-and-power, 2) increasing mean-time-between-failure, and 3) reducing system complexity.

Beam steering based on liquid crystal (LC) optical phase array (OPA) has been demonstrated by Raytheon and Hughes since the 1980s. OPA has micro-radian precision, high diffraction efficiency and negligible side lobes, but its scanning angle is limited. To widen steering angle, one coarse OPA and one fine OPA are cascaded. For two-dimensional beam steering, two OPAs arranged in orthogonal directions are commonly used.

Recently, Vescent Photonics developed a new *refractive* beam steering device using a LC material as a cladding layer in a slab waveguide. The evanescent field of the fundamental waveguide mode interacts with the LC layer near the surface of the waveguide where the LC molecules are well-ordered (low loss) and experience high restoring forces (<0.5 ms response time) and large steering angle. The major challenge of Vescent's beam steering device (SEEOR) is its relatively long optical beam path. In the VIS and NIR spectral regions, most liquid crystals have negligible absorption so that the absorption loss is minimal. In the MWIR and LWIR regions, some closely overlapped molecular vibration bands exist. As a result, the baseline absorption coefficient of 5CB reaches 10/cm. In a 2π-modulo OPA, the employed LC layer is usually thinner than 10 μm. Thus, the absorption loss is ~1%. But in Vescent's SEEOR, the optical path length could range from 50 μm to 1 mm and the absorption loss could be significant. Thus, there is an urgent need to develop low-loss liquid crystals in order to extend SEEOR operation to MWIR and LWIR.

2. Technical Approach

A major challenge for IR applications of liquid crystals is the inherently large absorption loss due to some overlapping molecular vibration bands and their overtones. In the off-resonance regions, the baseline absorption coefficient of 5CB (cyano-biphenyl) reaches as high as α~10/cm [ST Wu, J. Appl. Phys. 84, 4462 (1998)]. The transmittance (T) of a liquid crystal layer can be expressed as

$$T = e^{-\alpha d}, \tag{1}$$

where α is the absorption coefficient and d is the LC layer thickness. Let us take α~10/cm as an example. For a 10-μm-thick LC layer, αd=0.01 and the transmittance remains 99%. However, if the LC layer thickness (or effective optical path length) increases, then the absorption will increase exponentially, as Eq. (1) indicates. To improve transmittance, two approaches are commonly pursued: 1). To minimize absorption coefficient α by selecting proper functional groups, while maintaining nematic phase; 2). To reduce the cell gap d or optical path length by using a high birefringence LC material. Here we define a figure-of-merit (*FoM*) to compare the performance of an LC:

$$FoM = \frac{\Delta n}{\alpha}. \tag{2}$$

The molecular vibration frequency (ω) of a diatomic group depends on the spring constant (κ) and the effective mass (m) as:

$$\omega = \sqrt{\kappa/m}. \tag{3}$$

As the effective mass increases the vibration frequency decreases, i.e., the absorption band shifts toward a longer wavelength. Table 1 shows some common absorption bands that occur in MWIR and LWIR regions: e.g., CH stretching, CN stretching, C=C stretching in phenyl rings, C-H in-plane deformation, C-C skeletal stretching, C-F stretching, and C-H out-of-plane deformation.

Table 1: IR absorption of different functional groups in typical liquid crystals.
(str.=stretching; s.=strong absorption; m.=medium absorption; def.=deformation; w.=weak absorption; v.=variable intensity) [B. D. Mistry, *A Handbook of Spectroscopic Data: Chemistry-UV, IR, PMR, CNMR and Mass Spectroscopy,* Oxford, 2009]

	Vibration mode	Frequency (cm^{-1})	Wavelength (µm)	Relative intensity
C-H in phenyl ring	str.	3095-3010	3.23-3.32	m.
-CH_2-, -CH_3	str.	2950-2845	3.39-3.51	m.
C≡N	str.	2185-2120	4.58-4.72	s.
C≡C (non terminal)	str.	2260-2190	4.42-4.57	very weak
C-H in phenyl ring	str. overtone	1850-1780	5.40-5.62	m.
C=C	str.	1625	6.16	v.
C-H in -CH_2-	def.	1485-1445	6.74-6.92	m.
C-H in -CH_3	def.	1470-1430	6.80-7.00	m.
C-H in phenyl ring	in-plane def.	1225-950	8.16-10.53	w.
C-C	skeletal str.	1300-700	7.69-14.29	m.
C-F	str.	1100-1000	9.01-10.00	s.
-CF_2-	str.	1250-1050	8.00-9.50	s.
-CF_3	str.	1400-1100	7.14-9.10	s.
C-Cl	str.	800-600	12.5-16.67	s.
C-H in phenyl ring	out-of-plane def.	900-670	11.11-14.93	w.

More specifically, in the MWIR region the following absorption bonds dominate: the C-H stretching in a phenyl ring, -CH_2- and -CH_3 stretching from an alkyl chain, C≡N stretching from the cyano polar group, and some overtones from in-plane and out-of-plane C-H deformations. On the other hand, in the LWIR region following absorption bands dominate: C-H in-plane and out-of-plane stretching, C-C skeletal stretching, and C-F stretching.

From Eq. (3), three approaches can be considered to shift the absorption bands outside the spectral region of interest: deuteration, fluorination, and chlorination.

1) Deuteration: Substituting hydrogen with deuterium doubles the effective mass. As a result, the molecular vibration frequency would shift toward a longer wavelength by a factor of $\sqrt{2}$. The C-D in-plane and out-of-plane deformations would occur outside the LWIR region. However, deuteration shifts the C-H vibration in alkyl chain (~3.5 µm) to ~4.8 µm [ST Wu, et al. J. Appl. Phys. 92, 7146 (2002)]. *Therefore, to reduce absorption for both LWIR and MWIR bands we should do deuteration only for the phenyl rings, but not for the alkyl chain.*

4

2) Fluorination: As shown in Table 1, the vibration frequencies of CF, CF_2 and CF_3 occur in the LWIR region. *Therefore, fluorination could be favorable for MWIR but is unfavorable for LWIR.* However, a special caution must be taken. From Table 1, the overtones of CF, CF_2 and CF_3 could appear in the MWIR region. This is indeed observed in our recent studies of fluorinated terphenyl liquid crystal in the MWIR region [Y. Chen, et al. Opt. Express 19, 10843 (2011)]. Although the overtone intensity is reduced significantly, it is still noticeable especially when the optical path length is long.

3) Chlorination: As shown in Table 1, the C-Cl vibration frequency occurs at 800-600 cm^{-1}, which is outside the LWIR band. Moreover, its overtone will not show up in the MWIR region. Therefore, from an absorption viewpoint C-Cl seems to be a better polar group than CN and CF. We have previous experiences in chlorinated liquid crystals [ST Wu, et al. Liq. Cryst. 10, 635 (1991)], but not aimed for IR applications. Here we report some new chloro LC compounds with special emphasis on low IR absorption.

3. Progress

3.1 Benchmark: 5CB

In our study, a well-studied liquid crystal 5CB is used as benchmark, whose chemical structure is shown in the inset of Fig. 1. We measured the absorption coefficient of 5CB (in an isotropic phase) using FTIR (Spectrum Two, Perkin Elmer).
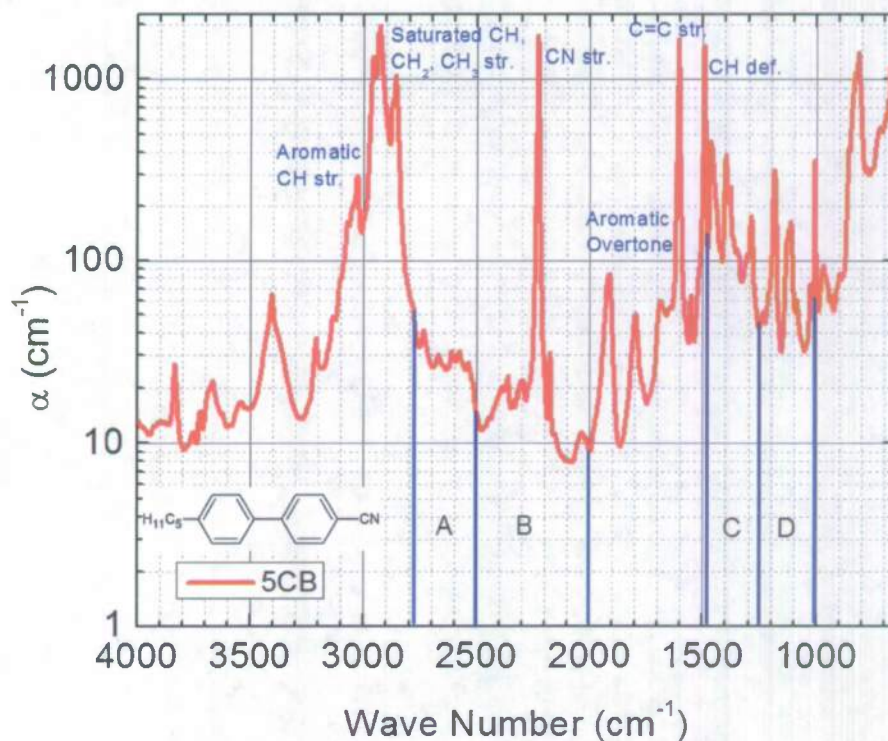
Fig. 1: Measured absorption coefficient of 5CB.

Figure 1 depicts the measured absorption coefficient of 5CB from 4000 cm^{-1} to 650 cm^{-1}. The C-H stretching band (including $-CH_2$ and $-CH_3$) is quite broad (3300-2800 cm^{-1}) and strong, and the peak absorption coefficient exceeds 600 cm^{-1}. In the center of MWIR (2500 cm^{-1} to 2000

cm^{-1}, marked as Zone B in Fig. 1), the C≡N stretching shows a narrow but very strong absorption (α>1000 cm^{-1}). Cyano is a strong polar group, which not only provides a large dielectric anisotropy but also extends the conjugation length for enhancing birefringence. For practical applications, a large $\Delta\varepsilon$ helps to reduce operation voltage while high Δn enables a thinner LC layer to be used for reaching the required phase change. Unfortunately, C≡N has a strong absorption at λ=4.45 μm and should be avoided because it will lift up the baseline absorption. A molecular vibration band usually has Lorentzian shape and its tail could spread broadly. The overlap of the neighboring bands is responsible for the observed baseline absorption.

Besides the normal vibration mode of C≡N, the baseline absorption in Zone B also comes from the overtone (doubled frequency) of the absorption bands in Zone D, as marked in Fig. 1. As listed in Table 2, the C-C (in the alkyl chain) skeletal stretching (1300-700 cm^{-1}) and the in-plane deformation of C-H in the phenyl rings (1225-950 cm^{-1}) contribute to the absorption in Zone D. The absorption of Zone C consists of the -C-H (in alkyl chain) deformation and C-C skeletal stretching, whose overtone further increases the baseline absorption observed in Zone A. The tail of the absorption band in Zone A may also raise the absorption level in Zone B.

In summary, the absorption in MWIR (Zones A and B) are primarily influenced by the strong C≡N stretching and the overtone/combination absorption from Zones C and D.

Table 2: Possible absorption mechanisms for Zones A-D shown in Fig. 1.

Zone	Absorption mechanism	Frequency (cm^{-1})	Wavelength (μm)
A	C-H (in CH$_2$, CH$_3$) def. overtone C-C skeletal str. overtone	2790-2500	3.58-5
B	C≡N str. C-H (in phenyl ring) in-plane def. overtone C-C (in alkyl chain) skeletal str. overtone Combination	2000-2500	4-5
C	C-H in CH$_2$, CH$_3$ def. C-C skeletal str.	1485-1250	6.73-8
D	C-H (in phenyl ring) in-plane. def C-C (in alkyl chain) skeletal str.	1000-1250	8-10

3.2 Fundamental modes
3.2.1. Undesirable polar groups: C≡N and NCS

As shown in section 3.1, C≡N has a strong absorption at λ=4.45 μm and should be avoided for broadband application. Besides C≡N group, NCS and C-F are two other commonly used polar groups. Compounds with different polar groups were prepared, dissolved in CCl$_4$ at a concentration of ~5x10^{-5} mol/ml and then filled in a NaCl cell with cell gap (0.5 mm). The transmission spectra were measured using FTIR, as shown in Fig. 2. NCS exhibits a very strong and broad absorption from 2220-1923 cm^{-1}, while C-F has an absorption band (1100-1000 cm^{-1}), which is outside the MWIR spectral region [Table 1].

Another polar group C-Cl can also be employed since its absorption is in the range of 800-600 cm^{-1}, and its second harmonic overtone will not show up in Zone B.
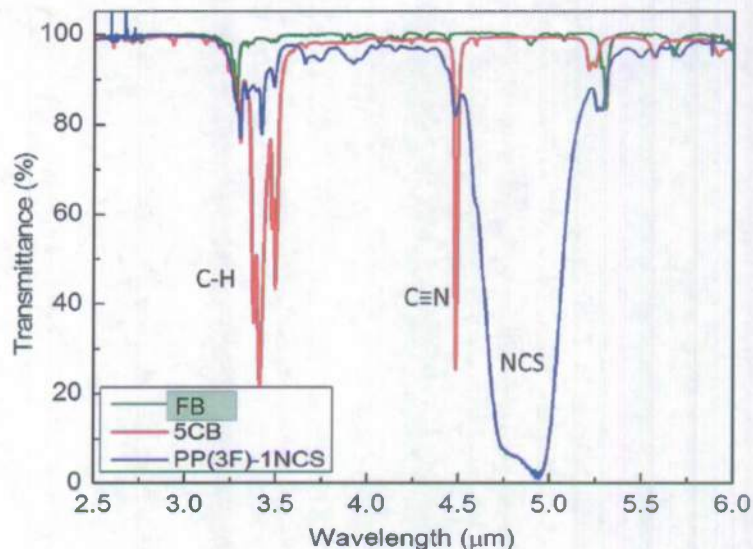
6

Fig. 2. Measured transmission spectra of three compounds with different polar groups. FB stands for F-Ph-Ph-F, where Ph is a phenyl ring.

3.2.2. Tolane

Tolane core is effective for elongating the conjugation length and enhancing birefringence. Theoretically, as a linking group C≡C exhibits a much weaker absorption than it is as a terminal group. We measured the absorption coefficient of a tolane compound PTP-20F, and results are depicted in Fig. 3. The absorption peak of C≡C occurs at 2216 cm^{-1} and its α is ~6X smaller than that of C≡N bond. However, this absorption peak raises the absorption baseline to >10cm^{-1} in the 2500-2000cm^{-1} region. Thus, C≡C is not a favorable linking group and should be avoided.
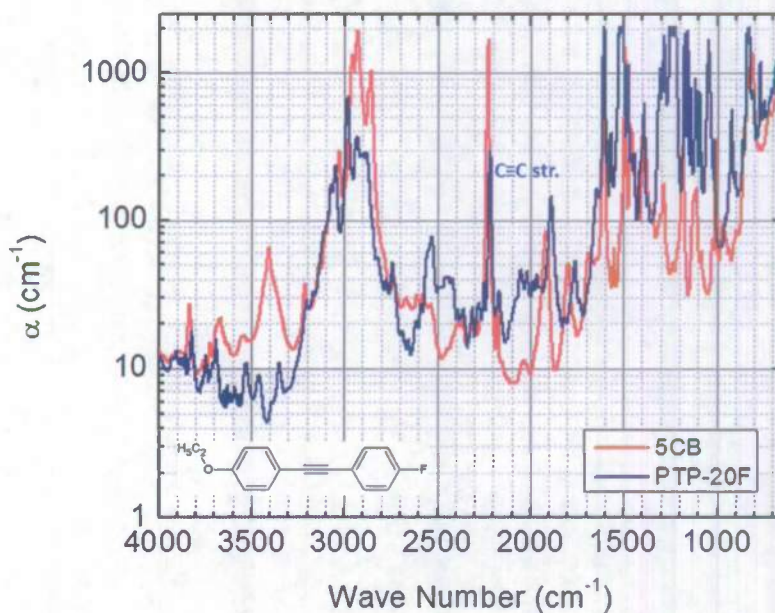
Fig. 3. Measured absorption coefficient of PTP-20F vs. 5CB.

3.3 Reducing overtone absorption

3.3.1. Avoiding C-O group

C-O group helps to stabilize mesongenic phase. The absorption of C-O group occurs at 1272-1200 cm^{-1}, but its overtone appears in 2540-2400 cm^{-1} [Fig. 3]. Therefore, we should avoid using C-O functional group.

3.3.2. Short alkyl chain

To study how alkyl chain affects the MWIR absorption, we measured the absorption coefficient of bi-phenyl compounds by FTIR. Figure 4 depicts the absorption spectrum of PP-2 and PP. The structures of PP-2 and PP are included in Fig. 4. Due to the absence of alkyl chain, PP shows lower absorption baseline in the whole IR region and the lowest absorption coefficient is less than 2 cm^{-1} at ~3500cm^{-1}. Both of them show a relatively strong resonance peak near 3000 cm^{-1}, which corresponds to the =C-H (in phenyl rings) stretching absorption. The absorption in 2950-2845 cm^{-1} comes from the –C-H (in alkyl chain) stretching absorption, which only occurs for PP-2. Besides that, PP also shows much lower overtone absorption in the spectrum region of interest 2500-2000 cm^{-1}. A shorter or even without alkyl chain will help reduce the absorption. But neither PP nor PP-2 has a LC phase. Flexible chain is favored to induce nematic phase. Thus, we need to compromise between the nematic phase and absorption when designing low-loss LCs.
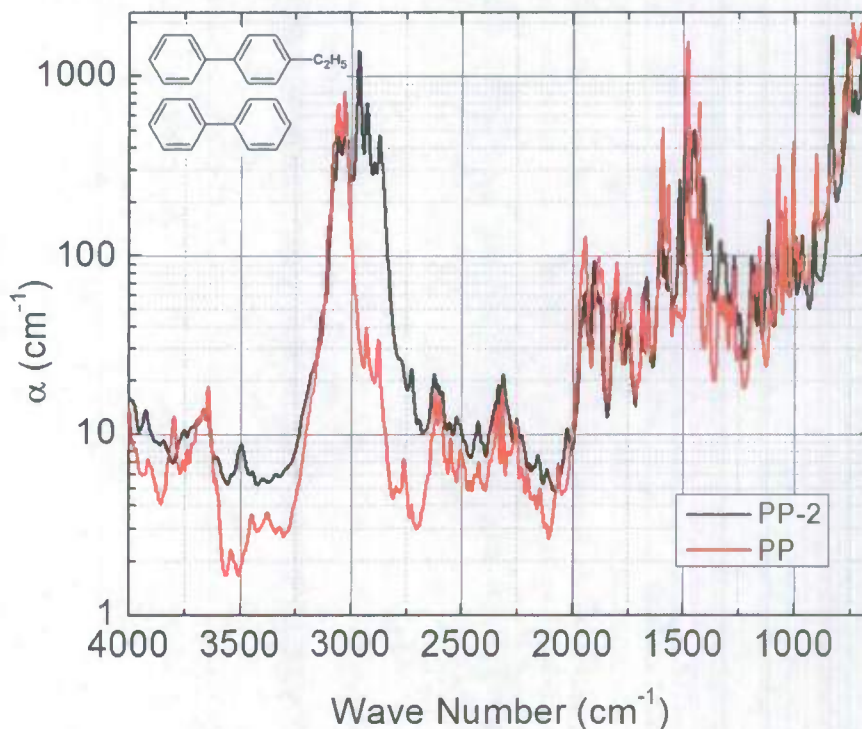
Fig. 4. Measured absorption coefficient of PP vs. PP-2.

Since the presence of alkyl tails results in larger absorption in the MWIR region, an extreme example is to eliminate all the alkyl chain, while keeping nematic phase. To ensure large aspect ratio for mesongenic phase, quaterphenyl compounds are investigated. As shown in Fig. 5,

8

without any alkyl chain, the first compound shows enantiotropic nematic phase. The quaterphenyl molecule without any substitution (the middle compound in Fig. 5) has high level of π-π interaction leading to efficient molecular packing. Such interaction results in high melting point [322 °C; Beilstein, J. Org. Chem. 9, 698–704 (2013)]. To lower the melting point and render the molecule useful for IR applications, disruption of the molecular packing is needed. Chlorine substitution can be used for reducing the ring coplanarity of the quaterphenyl molecule. By introducing one chlorine substitution, the melting point of the third compound drops 150 °C, compared to the second compound. The substitution position also matters in terms of the temperature range, and we will further study on this and find useful LC compound structures.

Cr 272°C N 310°C I   Cr 322°C I   Cr 172°C I
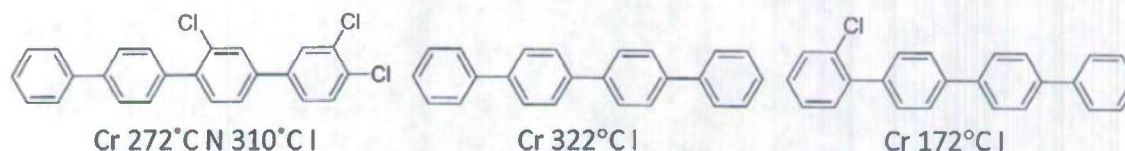
Fig. 5. Molecule structure and phase transition temperature of quaterphenyl molecules

3.3.3. Reducing =C-H in-plane deformation absorption

Phenyl ring is a very common group in LCs since it helps to increase Δn and it's more stable compared to tolane. But the in-plane deformation of =C-H (1225-950 cm^{-1}) in the phenyl rings occurs and its overtone contributes to the absorption in 2500-2000 cm^{-1}. For comparison, we measured the absorption spectrum of a compound with no unsaturated bonds 5CC2. 5CC2 has sematic phase from -16 °C to 77 °C and its chemical structure is shown in Fig. 6.
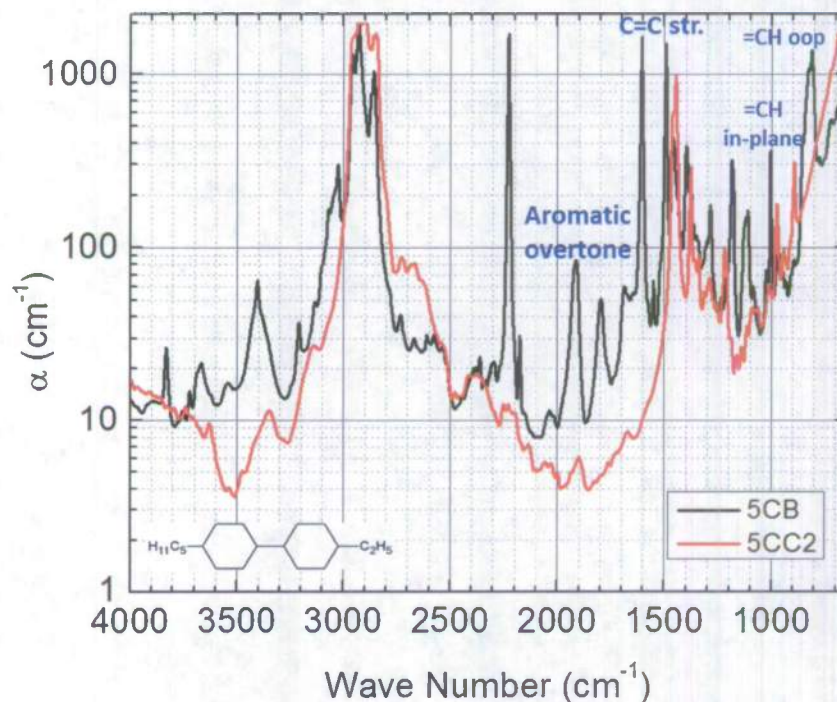

Fig. 6. Measured absorption coefficient of 5CC2 and 5CB.

9

From Fig. 6, the absorption of 5CC2 is very low from 2200-1700cm^{-1} due to the absence of aromatic overtone. For application in this spectral region, we may consider to use the saturated compounds. However, the birefringence is relatively low (~0.05). On the other hand, this study proves that the overtone of =C-H deformation contributes significantly to the absorption in 2500-2000 cm^{-1}. Proper substitution in the phenyl rings with F or Cl can decrease the number of =C-H bonds and hence reduce the in-plane deformation absorption. We will discuss about the fluorination and chlorination in the following two sessions respectively.

3.3.4. Fluorination

If a hydrogen atom in the phenyl ring is substituted by fluorine, the corresponding =C-F deformation will shift toward a longer IR region. The fundamental absorption of C-F stretching occurs at 1229 cm^{-1} and 1159 cm^{-1}, which are out of MWIR range. However, the overtone of this stretching could also contribute to the absorption in the 2500-2000 cm^{-1}. To quantitatively study this effect, we measured the absorption spectra of PP-2 and 2PPF, whose chemical structures are shown in the inset of Fig. 7. They have the same core structure and alkyl chain length, except there is a fluorine atom at the end of the phenyl ring for 2PPF. From Fig. 7, there are two strong additional absorption bands showing up at 1229 and 1159 cm^{-1}. And the overtone raises the absorption coefficient of 2PPF in the 2500-2000 cm^{-1} region, although only one fluorine atom is introduced. Thus, fluorination is not a good choice for lowering the absorption in the MWIR region because of its overtone absorption.
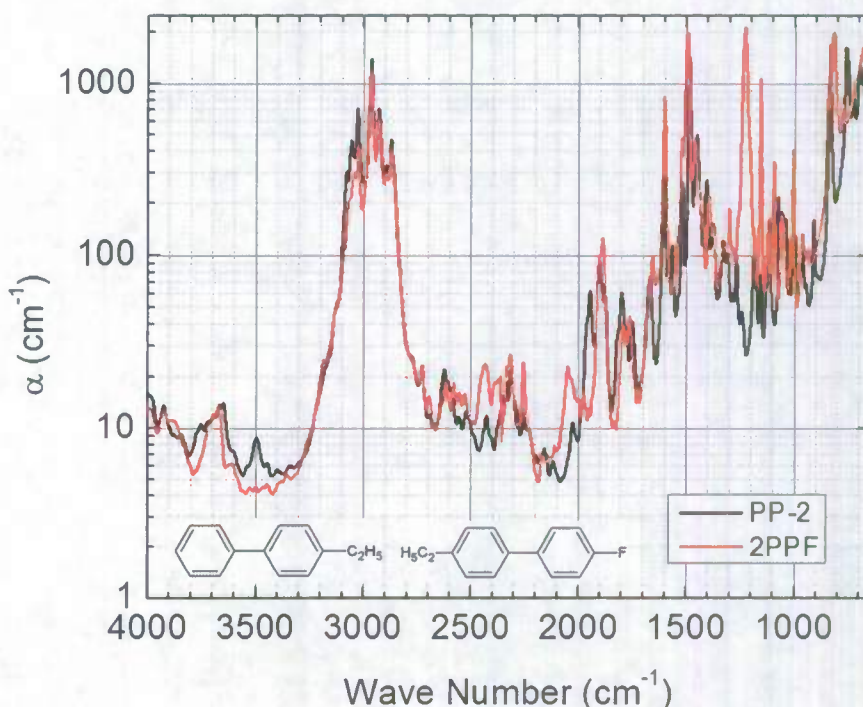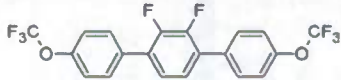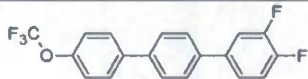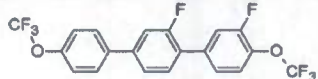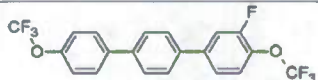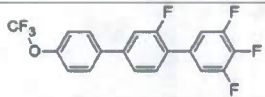

Fig. 7. Measured absorption coefficient of PP-2 vs. 2PPF.

However, the situation could change if we do complete fluorination in the alkyl chain because all the saturated –C-H bond stretching absorption at ~2900 cm^{-1} would shift to ~1100

cm^{-1} for the –C-F bond (stretching absorption). Thus, we could eliminate the strong and broad absorption in the 3000 to 2600 cm^{-1} region. One tradeoff is that fluoride atom is much heavier than hydrogen atom, and may suppress the liquid crystal phase or increase the melting point significantly. We did careful investigation and formed a eutectic mixture consisting of five fluorinated compounds without any alkyl chains. The chemical structures and properties are listed in the Table 3.

Table 3: Chemical structures and phase transition temperature of the fluorinated compounds in IR-01.

Comp.#	Chemical Structure	PTT (°C)	ΔH (cal/mol)
1		Cr 85.8 N 87.6 Iso	4921.0
2		Cr 85.5 N (83.6) Iso	5739.0
3		Cr 54.69 N (40.4) Iso	4820.7
4		Cr 113.4 Iso	4800.9
5		Cr 66.1 Iso	6583.7
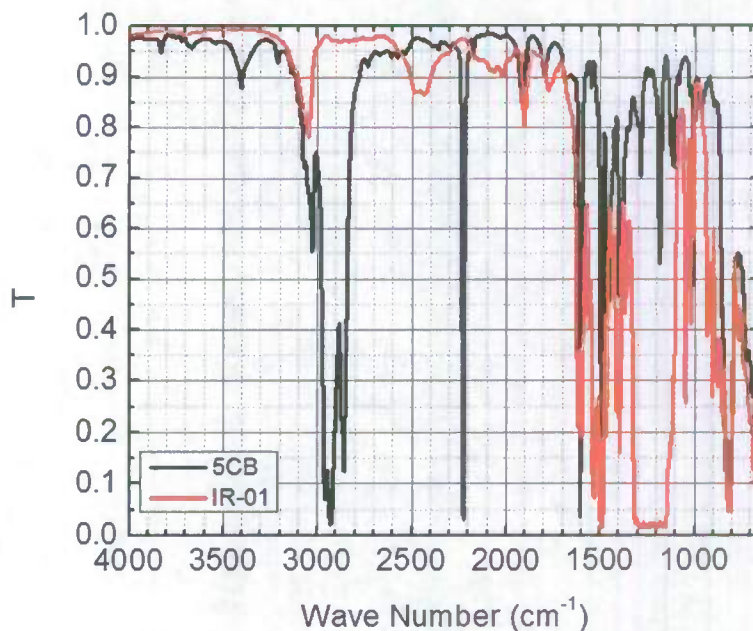
Fig. 8. Transmission spectra of a 20-μm liquid crystal layer of 5CB and IR-01.

11

The mixture has a clearing point of 51.5 °C and its melting point is lower than -10 °C due to super-cooling effect. We also measured its transmission spectrum in the IR region, as depicted in Fig. 8. The transmission spectrum of 5CB is also included for comparison. IR-01 does not have long alkyl chain as 5CB does, so it shows a much higher transmittance in the 3000-2600 cm^{-1} region. Besides, it also has a relatively high transmittance at 2227 cm^{-1} due to the absence of CN bond. However, there is a modest absorption band near 2400 cm^{-1}, which is contributed by the overtone of the -CF_3 stretching absorption. For application in 2500-2000 cm^{-1}, this is not desirable. But here we demonstrated a concept that we could engineer the absorption spectrum for application in a specific spectral region by carefully designing the molecular structure while keeping a reasonably wide nematic phase.

3.3.5. Chlorination

Besides fluorination, chlorination in the phenyl ring is another option to shift the =C-H in-plane deformation absorption to a longer wavelength. Based on Eq. (3), since chloride has even heavier atomic mass, the C-Cl stretching absorption occurs at 650 cm^{-1}, whose second harmonic absorption would locate outside of the 2500-2000 cm^{-1} region. Figure 9 shows the absorption spectrum of 2PPCl. The baseline of the 2PPCl is much lower than that of 5CB due to the shorter alkyl chain and the absence of CN group. The lowest absorption coefficient is ~4 cm^{-1} at ~2150 cm^{-1}. Thus, chlorination is an effective way to achieve low absorption in MWIR.
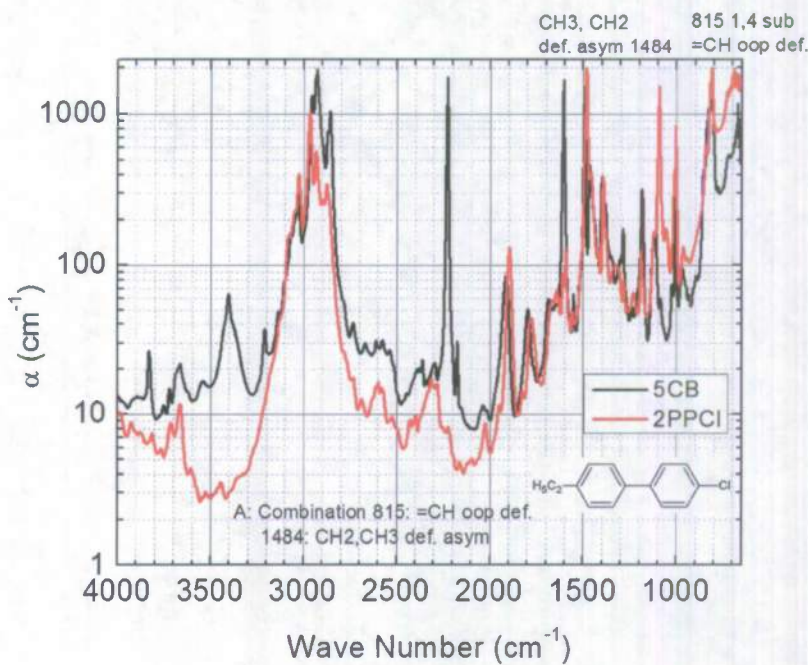

Fig. 9. Measured absorption coefficient of 5CB and 2PPCl.

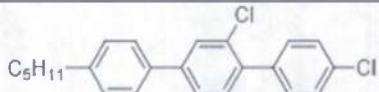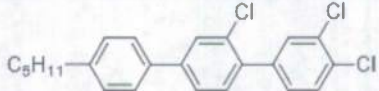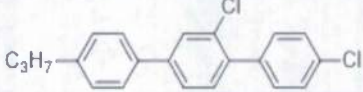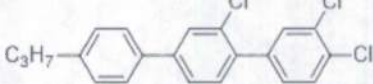### 3.3.6. Reducing combination absorption

From Fig. 9, we noticed that there is an unexpected absorption peak near 2300 cm^{-1}. It's not corresponding to any second harmonic absorption. We suspect that it might result from higher order overtone or combination absorption of lower frequency (sum frequency). $-CH_2$ and $-CH_3$

(in alkyl chain) asymmetric deformation occurs at ~1484 cm^{-1}, and =C-H (in phenyl ring) out-of-plane deformation contributes to the strong peak at ~815 cm^{-1}. The sum frequency of these two absorption bands is speculated to cause the absorption at ~2300 cm^{-1}. The combination absorption is difficult to predict, but the magnitude is much smaller compared to the fundamental absorption. But if the optical path is long (cm), this small absorption coefficient could still be quite significant.

3.4 Low absorption LC compounds

Based on the analysis of the absorption mechanism mentioned above, we ruled out the undesired functional groups and synthesized several chlorinated compounds whose structures and phase transition temperatures are listed in Table 4. All of these compounds exhibit a mesogenic phase.

Table 4: Chemical structures and phase transition temperature of the chlorinated compounds studied.

Comp.#	Name	Chemical Structure	PTT (°C)
6	ST 04 121		Cr 71 (N 65) Iso
7	ST 04 122		Nematic at room temperature
8	ST 04 128		Cr 95 (N 68) Iso
9	ST 04 129		Nematic at room temperature

If the employed LC has Δn~0.2, then the required cell gap for getting 2π phase change at λ=4µm is 20 µm. We measured the transmission spectrum of a 20-µm layer of each compounds from 4000 cm^{-1} to 650 cm^{-1} and compared to that of 5CB. With similar functional groups, these four LC compounds exhibit similar absorption spectra, except that the shorter alkyl chain would result in a lower absorption. Figure 10 depicts the transmission spectrum of ST 04 121 as an example. ST 04 121 shows higher transmittance than 5CB in the spectral regions of 2700-1950 cm^{-1} and 3700-3200 cm^{-1}. For practical applications, we will synthesize more homologues for formulating eutectic mixtures with a wide nematic temperature range.
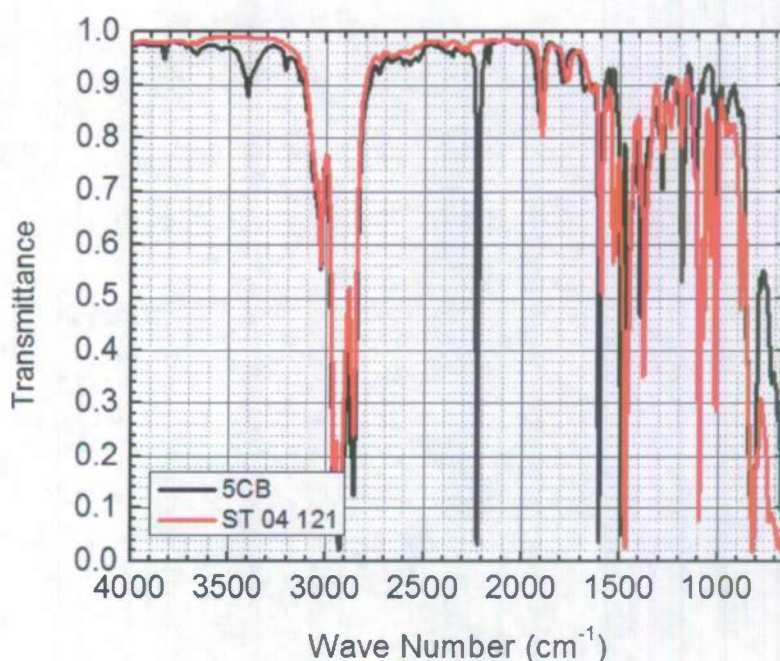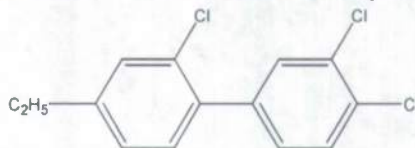
13

Fig. 10. Transmission spectra of a 20-μm liquid crystal layer of 5CB and ST 04 121.

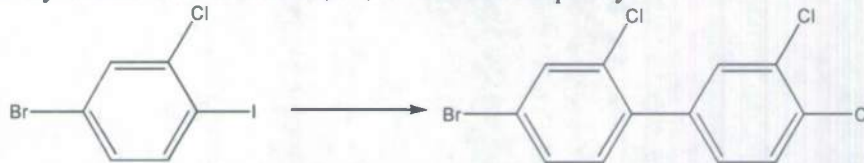## 3.5 Synthesis method and progress

3.5.1 Synthesis of chlorinated biphenyls

<u>Representative procedure:</u>

Synthesis of 2, 3', 4'-trichloro-4-ethyl biphenyl

1). 03014 KW Synthesis of 4-bromo -2, 3', 4'-trichloro biphenyl

In a 200 ml round bottom flask fitted with a magnetic stirbar was dissolved 4-bromo-3-chloroiodobenzene (3.17 g, 10.0 mmol) in a mixture of 16 ml H_2O and 40 ml 1,4-dioxane to give a colorless solution. Pd(PPh$_3$)$_4$ (115 mg, 1.0 mol%) and 3,4-dichlorophenylboronic acid (1.9 g, 1.0 equiv., 10.0 mmol) were added to the solution and the mixture was stirred at room temperature for 10 minutes. Potassium carbonate (5.52, 4.0 equiv.) was then added to the mixture and the reaction was refluxed for 48 hours. The reaction was monitored by TLC noticing the appearance of one new compound and the disappearance of the starting material. The mixture was poured to a 250 ml separatory funnel and the organic layer was separated. The aqueous layer was extracted with 60 ml ethyl acetate twice and the combined organic layer was washed with brine and dried with $MgSO_4$. Column chromatography (hexane as the eluent) was used to isolate

14

the desired product. (white solid, 2.2 g, 60 %)

^{1}H NMR (400 MHz, CDCl$_3$) δ: 7.63 (d, J = 2.4 Hz, 1H), 7.56 (d, J = 2.0 Hz, 1H), 7.30 (dd, J = 2.0 Hz, 1.6 Hz, 1H), 7.24 (s, 1H), 7.19 (d, J = 8.4 Hz, 1H), 7.10, (dd, J = 2.0 Hz, 1.6 Hz, 1H); ^{13}C NMR (400 MHz, CDCl$_3$) δ: 141.1, 137.8, 137.1, 133.4, 132.8, 132.5, 132.0, 131.2, 130.4, 129.2, 128.8, 123.2, 122.7.

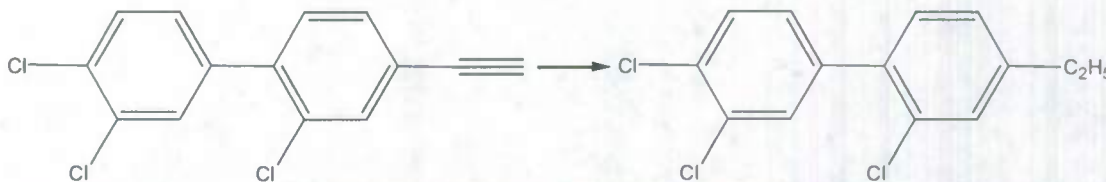2). 03015 KW Synthesis of 2, 3', 4'-trichloro-4-ethynyl biphenyl
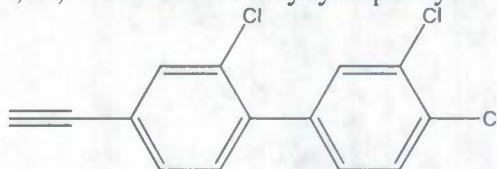
In a 250 ml pear flask fitted with a stirbar was added diisopropylamine (80.0 ml), triphenylphosphine, (79 mg, 6.0%), PdCl$_2$ (8.8 mg, 1.0 %) and CuI (4.8 mg, 0.8 %). The mixture was stirred in a ~60° oil bath for one and a half hours under a nitrogen atmosphere until all the orange salts dissolved. After cooling to room temperature, 4-bromo-2,3',4'-trichlorobiphenyl (1.68 g, 5.0 mmol) and trimethylsilylacetylene (1.5 ml, 10.0 mmol, 2.0 eq.) were added with the assistance of 4.0 ml diisopropylamine. The mixture was stirred at room temperature for 48 hours and a brown precipitate was observed in the flask. TLC indicated the formation of a new compound with similar R$_f$ value compared to the starting material. The reaction was quenched with 40 ml H$_2$O and the mixture was carefully transferred to a 250 ml separatory funnel. The organic layer was separated and the aqueous layer was extracted with 60 ml ethyl acetate twice. The organic layer was combined, dried with MgSO$_4$ and filtered by gravity and the filtrate was condensed to give a brown residue. The crude product was filtered through a short silica gel column eluented by hexane to give a colorless oil. (1.78 g, 53 %).

^{1}H NMR (400 MHz, CDCl$_3$) δ: 7.58 (d, J = 1.6 Hz, 1H), 7.52 (d, J = 2.0 Hz, 1H), 7.48 (d, J = 7.8 Hz, 1H), 7.39(dd, J = 1.6 Hz, 1.6 Hz, 1H), 7.27 (m, 1H), 7.21 (d, J = 8.0 Hz, 1H), 0.26 (s, 9H); ^{13}C NMR (400 MHz, CDCl$_3$) δ: 139.6, 133.5, 132.7, 132.4, 132.4, 131.2, 130.5, 130.1, 129.5, 128.8, 124.5, 102.9, 94.7, -0.17.

The product was then dissolved in 40 ml methanol and potassium carbonate (1.38 g, 2 equiv.) was added and the mixture stirred at room temperature for 5 hours. The reaction was quenched with 40 ml H$_2$O and the mixture was extracted with ether 100 ml twice. The organic portion was dried with MgSO$_4$, condensed by vacuum to give a light yellow solid. (980 mg, 70 %)

^{1}H NMR (400 MHz, CDCl$_3$) δ: 7.60 (d, J = 1.6 Hz, 1H), 7.51 (d, J = 2.0 Hz, 1H), 7.48 (d, J = 7.8 Hz, 1H), 7.42(dd, J = 1.6 Hz, 1.6 Hz, 1H), 7.25 - 7.23(m, 2H), 3.16 (s, 1H); ^{13}C NMR (400 MHz, CDCl$_3$) δ: 138.5, 133.7, 132.7, 132.4, 132.4, 131.2, 130.5, 130.1, 129.5, 128.8, 123.5, 84.2, 79.4.

3). 03019 KW Synthesis of 2, 3', 4'-trichloro-4-ethyl biphenyl

A suspension of 2, 3', 4'-trichloro-4-ethynyl-biphenyl (product of 03015 KW, 563 mg, 2.0 mmol) and palladium (10 wt% on activated carbon; 100 mg) in ethanol (5 ml) and methanol (5

ml) was stirred at room temperature under a hydrogen atmosphere (1 atm) for 24 hours. TLC analysis indicated the disappearance of the starting material and the formation of a new compound with smaller R_f value. The reaction mixture was filtered through a pad of Celite, and the filtrate was condensed to give a yellow crude product. The new compound was isolated by column chromatography eluted with hexane. (a colorless oil, 370 mg, 62 %)

^{1}H NMR (400 MHz, CDCl$_3$) δ: 7.52 (d, J = 2.0 Hz, 1H), 7.48 (d, J = 8.0 Hz, 1H), 7.31(s, 1H), 7.27 (dd, J = 2.0 Hz, 2.4 Hz, 1H), 7.20 (d, J =7.6 Hz, 1H), 7.14 (dd, J = 0.8 Hz, 0.8 Hz, 1H), 2.67 (q, J = 7.6 Hz, 2H), 1.26 (t, J = 7.6 Hz, 3H); ^{13}C NMR (400 MHz, CDCl$_3$) δ: 146.0, 139.3, 135.3, 132.1, 131.7, 131.4, 131.0, 130.0, 129.6, 129.5, 129.2, 128.6, 127.8, 127.5, 126.7, 126.4, 28.3, 15.3.GC/MS: cal. 285.60 found 285.86.

Table 5 lists several chlorinated biphenyls we synthesized for absorption test, which will help us better understand the absorption mechanism and design low-loss LC compounds.

Table 5. Synthesized chlorinated biphenyls

Notebook number	Structure	Phase transition phase
03019KW		none found in DSC
03018KW		none found in DSC
03021KW		N/A

3.5.2. Synthesis of chlorinated terphenyls

The ^{1}H and ^{13}C spectra were measured on a Bruker Avance 400 MHz spectrometer at 400.13, 100.61 MHz, respectively. The ^{1}H and ^{13}C NMR chemical shifts were referenced to TMS (0.0 ppm). The melting points were uncorrected. The progress of the reactions were monitored either by thin layer chromatography with plastic backed silica gel plates (Scientific adsorbents incorporated, Catalog # 79011), or by GC-MS [Finnigan trace GC ultra (Restek[TM] RTX-5 capillary column (30 m)) coupled with Finnigan PolarisQ mass spectrometer]. Infrared spectra were obtained using a Bruker Vector33 infrared spectrometer with an ATR probe. Differential scanning calorimetry (DSC) measurements were performed using a TA instruments differential scanning calorimeter 2920 at heating and cooling rates of 5°C per minute. Transition temperatures of the final products were measured using Mettler FP82HT hot-stage and FP90 control unit in conjunction with Nikon Eclipse E600 Pol polarizing microscope.

Most of the terphenyl compounds prepared here showed nematic behavior at or below room temperature. In some cases exact transition temperatures could not be determined due to hardware limitations.
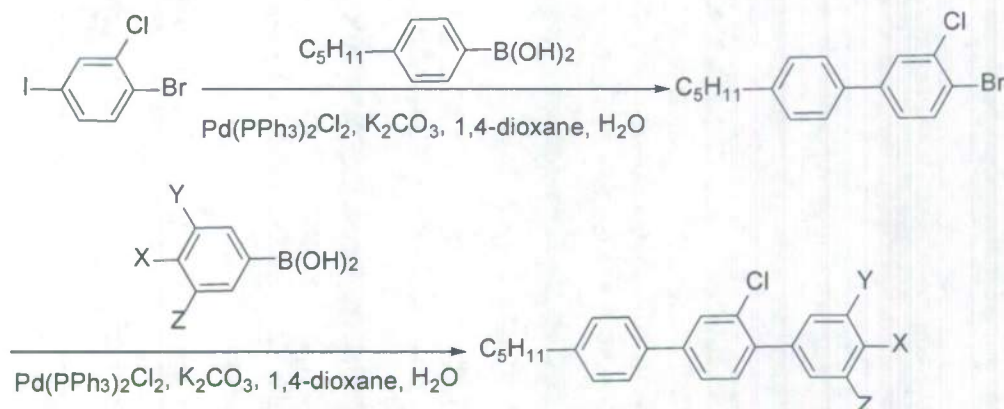
16

General synthesis scheme

Fig.11. Synthesis of chlorinated terphenyls with an alkyl tail (X =F, CF$_3$, OCF$_3$, Cl, CN, Y = F, Cl, H, Z = F, H)
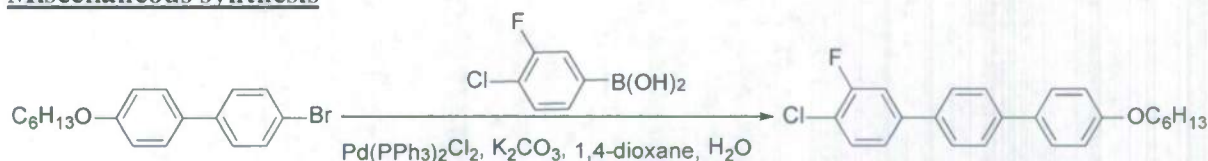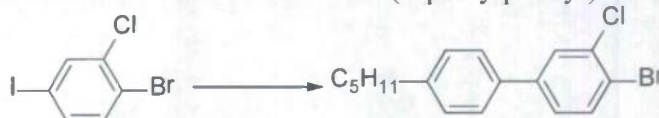
Miscellaneous synthesis

Fig. 12. Synthesis of 1-chloro-2-fluoro-4-{4-[4-(hexyloxy)phenyl]phenyl}benzene

Representative procedures

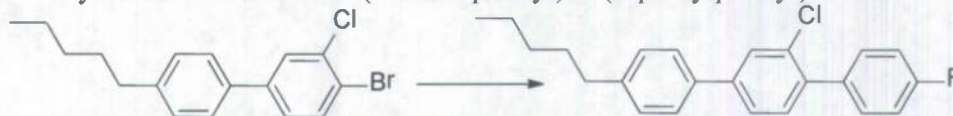Synthesis of 1-bromo-2-chloro-4-(4-pentylphenyl)benzene

In a 500 ml round-bottom flask K$_2$CO$_3$ (3.45 gm, 25 mmol) was dissolved in H$_2$O (40 ml) and 1,4-dioxane (100 ml) was added to it. This mixture was degassed by sonication under vacuum for 20 minutes and after that 4-pentylbenzeneboronic acid (2.028 gm, 10.56 mmol), 1-bromo-2-chloro-4-iodobenzene (3.348 gm, 10.56 mmol) and Pd(PPh$_3$)$_2$Cl$_2$ (160 mg, 3 mol%) was added to it. This mixture was refluxed for 18 hours under nitrogen when GC-MS showed complete conversion of the starting material. At this point, the mixture was cooled down to room temperature, adsorbed on silica gel and was placed on the top of a silica gel column. The column was eluted with hexanes and the major band was separated. The solvent was removed under reduced pressure to obtain the desired product as a colorless oil (2.20 gm, 62% yield).

^{1}H NMR (CDCl$_3$, 298 K, 400 MHz): 7.65 (1H, d, J = 4 Hz), 7.64 (1H, d, J = 10 Hz), 7.45 (2H, d, J = 8.4 Hz), 7.32 (1H, dd, J = 12 Hz, 2 Hz), 7.25 (2H, d, J = 8.4 Hz), 2.64 (2H, t, J = 7.6 Hz), 1.643 (2H, pent, J = 7.6 Hz), 1.38-1.30 (4H, m), 0.90 (3H, t, J = 8 Hz)

^{13}C NMR (CDCl$_3$, 298 K, 100 MHz): 143.22, 141.93, 136.07, 134.72, 134.27, 133.88, 129.09, 128.68, 126.75, 126.39, 120.83, 35.59, 31.51, 31.13, 22.56, 14.05

17

Synthesis of 2-chloro-1-(4-fluorophenyl)-4-(4-pentylphenyl)benzene
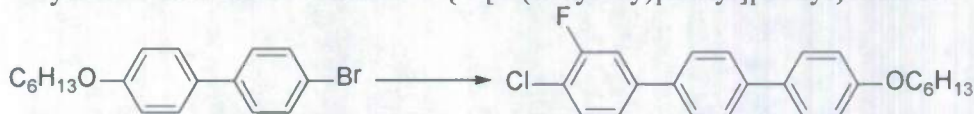

In a 250 ml round-bottom flask K_2CO_3 (2.76 gm, 20 mmol) was dissolved in H_2O (16 ml) and 1,4-dioxane (40 ml) was added to it. This mixture was degassed by sonication under vacuum for 20 minutes and after that 4-fluorobenzeneboronic acid (0.769 gm, 5.5 mmol), 1-bromo-2-chloro-4-(4-pentylphenyl)benzene (1.64 gm, 4.85 mmol) and $Pd(PPh_3)_2Cl_2$ (0.073 gm, 3 mol%) was added to it. This mixture was refluxed for 24 hours under nitrogen when GC-MS showed full conversion of the starting materials. At this point, the mixture was cooled down to room temperature, adsorbed on silica gel and was placed on the top of a silica gel column. The column was eluted with hexanes and the major band was separated. The solvent was removed under reduced pressure to obtain a viscous liquid. This was subjected to kugelrohr distillation (150°C, 0.5 millibar) and the residue was collected (not the distillate) to obtain a viscous white liquid (1.01 gm, 59% yield). As this compound is nematic near room temperature, recrystallization is difficult. In order to obtain high quality material, the material was subjected to silica gel column chromatography three times with hexanes as eluent and then kept under vacuum (0.3 millibar, 90°C) for 2 hours.

^{1}H NMR (CDCl$_3$, 298 K, 400 MHz): 7.69 (1H, d, J = 1.8 Hz), 7.52 (3H, d, J = 8.04 Hz), 7.48-7.42 (2H, m) 7.36 (1H, d, J = 7.96 Hz), 7.27 (2H, d, J = 8.32 Hz), 7.13 (2H, t, J = 8.76 Hz), 2.65 (2H, t, J = 7.76 Hz), 1.66 (2H, pent, J = 7.47 Hz), 1.41-1.30 (4H, m), 0.91 (3H, t, J = 7.00 Hz)
^{13}C NMR (CDCl$_3$, 298 K, 100 MHz): 163.60, 142.97, 141.91, 137.84, 136.60, 131.67, 131.56, 131.22, 131.14, 129.33, 129.04, 128.31, 128.10, 126.86, 125.39, 115.16, 114.95, 35.61, 31.55, 31.15, 22.57, 14.05

Synthesis of 1-chloro-2-fluoro-4-{4-[4-(hexyloxy)phenyl]phenyl}benzene

In a 100 ml round-bottom flask K_2CO_3 (2.208 gm, 16 mmol) was dissolved in H_2O (16 ml) and 1,4-dioxane (40 ml) was added to it. This mixture was degassed by sonication under vacuum for 20 minutes and after that 4-chloro-3-fluorobenzeneboronic acid (0.460 gm, 2.64 mmol), 4-bromo-4'-hexyloxybiphenyl (0.66gm, 2 mmol) and $Pd(PPh_3)_2Cl_2$ (0.040 gm, 3 mol%) was added to it. This mixture was refluxed for 24 hours under nitrogen when TLC (hexanes) showed full conversion of the starting materials. At this point, the mixture was cooled down to room temperature, adsorbed on silica gel and was placed on the top of a silica gel column. The column was eluted with hexanes and the major band was separated. The solvent was removed under reduced pressure to obtain a white solid (0.24 gm, 95% yield).
Mesogenic behavior: Cr 158 SmX 190 I
^{1}H NMR (CDCl$_3$, 298 K, 400 MHz): 7.63-7.52 (6H, m), 7.46-7.20 (3H, m), 6.97 (2H, d, J = 8.8 Hz), 3.99 (2H, t, J = 6.4 Hz), 1.80 (2H, pent, J = 6.8 Hz), 1.50-1.32 (6H, m), 0.90 (3H, t, J = 6.8 Hz)
^{13}C NMR (CDCl$_3$, 298 K, 100 MHz): 159.60, 159.03, 157.14, 141.43, 137.04, 132.56, 130.83, 128.03, 127.23, 123.18, 115.02, 114.91, 114.80, 68.15, 29.27, 25.75, 22.62, 14.05

We have synthesized several chlorinated terphenyls, which exhibit liquid crystal phase and low MWIR loss, as listed in Table 4.

3.5.3. Synthesis of chlorinated quaterphenyls

The ^{1}H and ^{13}C spectra were measured on a Bruker Avance 400 MHz spectrometer at 400.13 and 100.61 MHz, respectively. The ^{1}H and ^{13}C NMR chemical shifts were referenced to TMS (0.0 ppm. The melting points were uncorrected. The progress of the reactions were monitored either by thin layer chromatography with plastic backed silica gel plates (Scientific adsorbents incorporated, Catalog # 79011), or by GC-MS [Finnigan trace GC ultra (Restek^{TM} RTX-5 capillary column (30 m)) coupled with Finnigan PolarisQ mass spectrometer]. Infrared spectra were obtained using a Bruker Vector33 infrared spectrometer with an ATR probe. Differential scanning calorimetry (DSC) measurements were performed using a TA instruments differential scanning calorimeter 2920 at heating and cooling rates of 5°C per minute. Transition temperatures of the final products were measured using a Mettler FP82HT hot-stage and FP90 control unit in conjunction with Nikon Eclipse E600 Pol polarizing microscope.

General synthesis scheme

The preliminary set of quaterphenyls was prepared by Suzuki coupling between a custom synthesized bromobiphenyl unit and a biphenylboronic acid. As such, addition of substituents is initially restricted to two of the four quaterphenyl rings, as shown in Fig. 13.
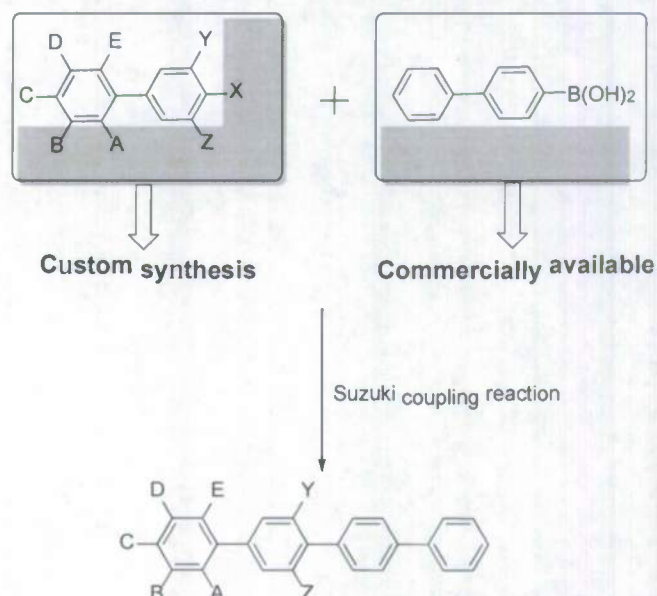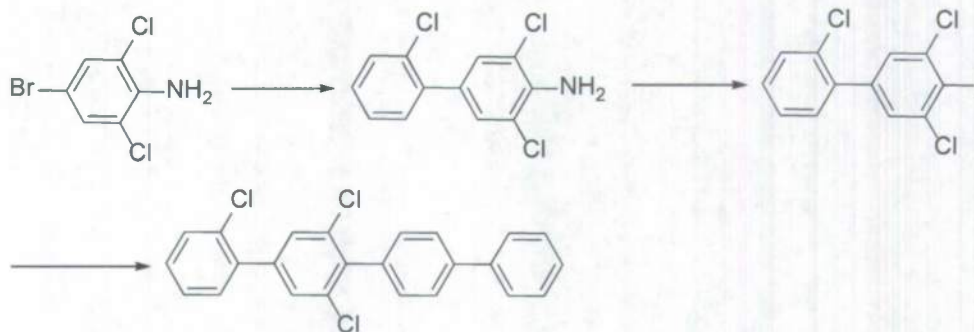

Fig. 13. Synthesis of chlorinated quaterphenyls devoid of alkyl tail (X =Br, I, Y = Cl, H, Z = Cl, H, A= Cl, H, B= Cl, H, C= Cl, H, D= Cl, H, E= Cl, H).
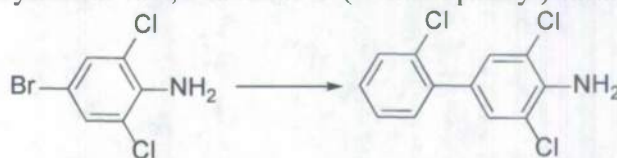
Representative procedure

Synthesis of 1,3-dichloro-5-(2-chlorophenyl)-2-(4-phenylphenyl)benzene

Stepwise procedure

### Synthesis of 2,6-dichloro-4-(2-chlorophenyl)aniline

In a 250 ml round bottom flask equipped with a stir bar was added PEG-2000 (10.5 gm) and Na_2CO_3 (2.11 gm, 20.0 mmol). After adding water (9 ml) the mixture was stirred at 50°C until it became a smooth viscous mass. Then $Pd(OAc)_2$ (22 mg, 1 mol%) was added under N_2 and the mixture was stirred for 5 minutes. Finally 4-bromo-2,6-dichloroaniline (2.409 gm, 10.0 mmol) and 2-chlorophenylboronic acid (2.34 gm, 15.0 mmol) were added to it all at once. The mixture was stirred for 12 hours when all the starting materials were consumed (monitored by GC-MS). The mixture was cooled down to room temperature and extracted with ether (3×100 ml). The combined organic layers were dried over $MgSO_4$ and the solvent was removed under reduced pressure to obtain a red liquid (2.99 gm). The GC-MS showed that the liquid is mostly the desired amine with very little amount of bi-products. The crude biphenyl was used immediately in the next reaction without any further purification.

Synthesis of 1,3-dichloro-5-(2-chlorophenyl)-2-iodobenzene
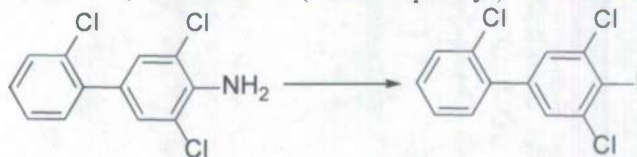
To a solution of p-TsOH·H_2O (5.73 g, 30.0 mmol) in MeCN (40 mL) was added 2,6-dichloro-4-(2-chlorophenyl)aniline (2.72 gm, 10.0 mmol). The resulting suspension of amine salt was cooled to 10–15 °C and to this was gradually added a solution of $NaNO_2$ (1.38 gm, 20.0 mmol) and KI (4.15 gm, 25.0 mmol) in H_2O (6 mL). The reaction mixture was stirred for 10 min then allowed to come to 20 °C and stirred until all the amine was consumed (GC-MS). Sodium thiosulfate (2 gm) was added to this mixture and then the mixture was adsorbed on silica gel and placed on the top of a silica gel column. The column was eluted with hexanes and the major band was separated to obtain the desired product as a light orange solid (3.23 gm, 84% yield). The GC-MS showed that it had very little amount of impurity and so it was used in the subsequent reaction without any further purification.

Synthesis of 1,3-dichloro-5-(2-chlorophenyl)-2-(4-phenylphenyl)benzene
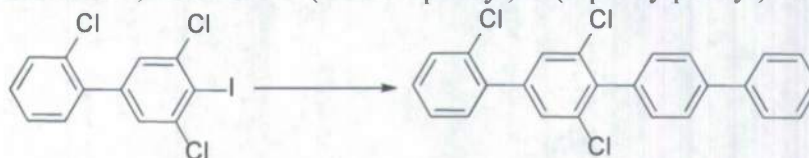
In a 100 ml round-bottom flask K_2CO_3 (0.69 gm, 5.0 mmol) was dissolved in H_2O (8 ml) and 1,4-dioxane (20 ml) was added to it. This mixture was degassed by sonication under vacuum for 20 minutes and after that biphenylboronic acid (0.742 gm, 3.75 mmol), 1,3-dichloro-5-(2-chlorophenyl)-2-iodobenzene (0.958 gm, 2.5 mmol) and $Pd(PPh_3)_2Cl_2$ (20 mg, 1.5 mol%) was added. This mixture was refluxed for 18 hours under nitrogen when TLC (eluent hexanes) showed complete conversion of the starting materials. At this point, the solvent was removed under reduced pressure and the residue was dissolved in boiling toluene and Montmorillonite K10 clay was added to it. The mixture was gravity filtered while hot and the filtrate was removed under reduced pressure to obtain a viscous liquid. Cold ethanol (75 ml) was added to this and a white solid precipitated out. The solid was separated by suction filtration to yield the desired product (0.475 gm, 46% yield).
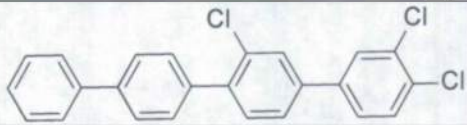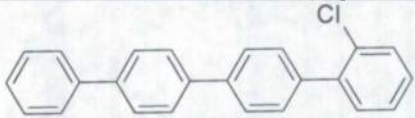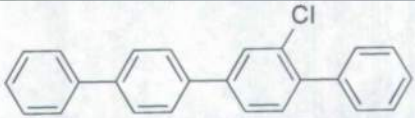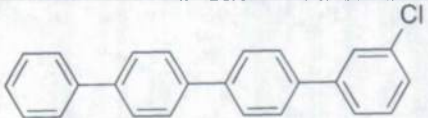
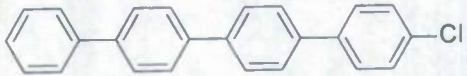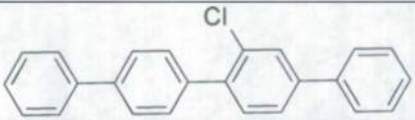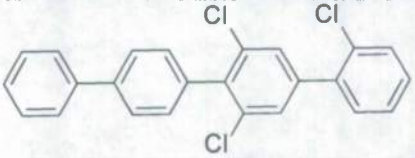Phase transition: Cr 163 I (This does not crystallize again on cooling even to -60°C)
^{1}H NMR (CDCl$_3$, 298 K, 400 MHz): 7.71 (2H, d, J = 8.8 Hz), 7.69-7.66 (2H, m), 7.51 (2H, s), 7.50-7.32 (9H, m)
^{13}C NMR (CDCl$_3$, 298 K, 100 MHz): 140.93, 140.49, 135.58, 134.58, 131.11, 130.24, 130.13, 129.54, 129.08, 128.80, 127.48, 127.20, 127.13, 126.92

Table 6 summarizes the synthesized quaterphenyls and their phase transitions. Several compounds exhibit liquid crystal phase. We will formulate eutectic mixture to lower the melting point. Without any alky chains, these compounds should have low absorption in MWIR.

Table 6. Phase transitions of the synthesized quaterphenyls

Notebook number	Structure	Phase transition
ST 04 139		Cr 272 N 310 I
ST 04 149		Cr 172 N 182 I
ST 04 151		Cr 164 I
ST 04 152		Cr 242 N 256 I
ST 05 003		Cr 334 N 348 I
ST 05 010		Cr 148 ?? 162 I
ST 05 002		Cr 163 I

4. Future work

4.1. MWIR

In the future, we will further develop more chlorinated compounds with nematic phase and low absorption coefficient in MWIR or high birefringence for thin cell operation. We will characterize the physical properties and evaluate the FoM of these compounds. Then we will formulate eutectic mixture to widen the nematic temperature range with these low absorption and/or high birefringence LC compounds.

On the other hand, we will investigate the alkyl-chain-free quarterphenyl compounds. We will study the chlorine substitution (number and position) effects on the phase transition temperature and hope to obtain low temperature liquid crystal compounds and formulate eutectic mixture with low MWIR absorption.

When the mixture is ready, we plan to deliver our low-loss and high birefringence LC mixture to Vescent Photonics or Raytheon for device testing.

4.2. LWIR

The =C-H in-plane deformation in the phenyl ring is the main cause for strong absorption near 10.6 μm. *Deuteration in the phenyl ring only* should shift this absorption band toward the longer wavelength side, which is outside the LWIR region. [S.T. Wu et al, J. Appl. Phys. 92, 7146 (2002)] From Table 1, the -C-H deformations in alkyl chain occur around 1430-1485 cm^{-1}. Deuteration on alkyl chain may shift this band to 1000 cm^{-1}, which is undesirable. Therefore, we propose to synthesize the two series of LC compounds, shown in Fig. 14 and formulate eutectic mixtures to achieve a wide nematic range.
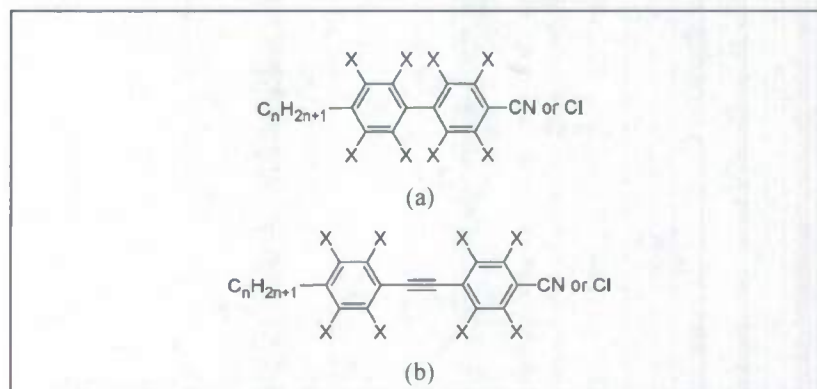

Fig. 14. Proposed low absorption compounds for LWIR, X=D or Cl.

4.3. SWIR

Liquid crystals with low absorption in MWIR usually exhibit low absorption in SWIR, since the absorption in SWIR results from the overtone or combination of the absorption in MWIR. This concept has been proven by comparing the absorption of 5CB and D5CB in SWIR region [ST Wu, et al. J. Appl. Phys. 92, 7146 (2002)]. We also plan to measure the SWIR absorption of our low-loss LC mixture designed for MWIR.